Weakly Nonlinear Convection in a Porous Layer with Multiple Horizontal Partitions

D. Andrew S. Rees[(1)] · **Andrew P. Bassom**[(2)] · **G. Genç**[(3)]

[(1)] *Department of Mechanical Engineering, University of Bath, Bath BA2 7AY, UK.*
[(2)] *School of Mathematics and Statistics, University of Western Australia, Crawley, WA 6009, AUSTRALIA.*
[(3)] *Department of Energy Systems Engineering, University of Erciyes, 38039, Kayseri, TURKEY.*

[(1)] D.A.S.Rees@bath.ac.uk
[(2)] andrew.bassom@uwa.edu.au
[(3)] gamzegenc@erciyes.edu.tr

Abstract We consider convection in a horizontally uniform fluid-saturated porous layer which is heated from below and which is split into a number of identical sublayers by impermeable and infinitesimally thin horizontal partitions. Rees and Genç (2011) determined the onset criterion by means of a detailed analytical and numerical study of the corresponding dispersion relation and showed that this layered system behaves like the single-sublayer constant-heat-flux Darcy-Bénard problem when the number of sublayers becomes large. The aim of the present work is to use a weakly nonlinear analysis to determine whether the layered system also shares the property of the single-sublayer constant-heat-flux Darcy-Bénard problem by having square cells, as opposed to rolls, as the preferred planform for convection.

Keywords Porous media · Layered medium · Convection · Weakly nonlinear theory · Pattern selection

NOMENCLATURE

A, B, C	roll amplitudes
c_1, c_2, c_3, c_4	constants in amplitude equations
c.c.	complex conjugate
$\mathcal{C}$	heat capacity
f, g	functions in weakly nonlinear theory
$\bar{g}$	gravity
h	height of sublayer
K	permeability
N	number of sublayers
p	pressure
P	disturbance pressure
Ra	Darcy-Rayleigh number
t	time
T	dimensional temperature
u, v	horizontal velocities
w	vertical velocity
x, y	horizontal coordinates
z	vertical coordinate

Greek symbols

α	disturbance wavenumber
β	expansion coefficient
γ	equal to d/δ
ΔT	reference temperature drop
ϵ	small quantity
θ	temperature
Θ	disturbance temperature
κ	thermal diffusivity
μ	dynamic viscosity
ρ	density
τ	slow time scale
ϕ	relative orientation of two rolls
Ω	coupling coefficient

Subscripts and superscripts

c	critical conditions
f	fluid
pm	porous medium
ref	reference value
$1, 2, 3, \cdots$	context-dependent meanings
$\hat{}$	dimensional quantity
$'$	derivative with respect to z

1 Introduction

It is well-known that the classical Darcy-Bénard layer admits thermoconvective instabilities once the Darcy-Rayleigh number exceeds $4\pi^2$; see Rees (2000, 2001), Tyvand (2002) and Nield and Bejan (2012). The corresponding wavenumber is π. In this case the two bounding surfaces are held at uniform but different temperatures with the lower surface being hotter. At slightly postcritical Darcy-Rayleigh numbers the preferred convective planform may be shown to consist of two-dimensional rolls by means of a weakly nonlinear analysis.

On the other hand, if the layer is heated from below by means of a constant heat flux and cooled from above in the same way, then the critical Darcy-Rayleigh number reduces to 12 and the critical wavenumber to zero. In this case the preferred slightly postcritical planform takes the form of square cells which are composed of two roll systems which are orientated at right angles to one another. This result may be inferred from the numerical studies of Riahi (1983) and Rees and Mojtabi (2011), although it is generally not widely known.

Rees and Genç (2011) considered a variant on the Darcy-Bénard problem where the layer was split into identical sublayers which are separated by infinitesimally thin impermeable interfaces. Thus the sublayers are decoupled in terms of the fluid flow, but heat may be transferred by conduction between the sublayers. The outer surfaces of the layer are again held at fixed but

different temperatures. Rees and Genç (2011) presented a detailed analysis of the onset problem by using dispersion relations. They found that, for a system consisting of N sublayers, the neutral curves bunch into very obvious families each containing N curves. In addition, the critical Rayleigh number and wavenumber decrease as N increases. More precisely they determined that these critical values have the following asymptotic forms,

$$Ra_c \sim 12 + 23.268397N^{-2}, \qquad k_c \sim 1.1055993\pi N^{-1/2}, \tag{1}$$

where the numerical values which arise in (1) are given precisely by,

$$24\Big(\frac{2}{21}\Big)^{1/2}\pi^2 \simeq 23.268397, \qquad \Big(\frac{21}{2}\Big)^{1/4}\pi^{1/2} \simeq 1.0155993\pi. \tag{2}$$

Therefore the critical values for the layer clearly approach those of the constant heat flux Darcy-Bénard layer even though the overall layer is heated by means of constant temperature boundary conditions. Given this, it is quite natural then to ask whether the stable planform for weakly postcritical convection changes from rolls to square cells as N increases since the latter planform arises for the constant heat flux single layer, and this is the aim of the present paper.

2 Problem Formulation and Basic State

We are investigating the effect of the presence of one type of layering on the identity of the weakly postcritical convection planform. The origin of the coordinate system is located at the very bottom of the layer with $\hat{x}$ and $\hat{y}$ being the horizontal coordinates and $\hat{z}$, the vertical coordinate. The composite layer is of infinite extent in both horizontal directions. When there are N sublayers present then the layer lies in the range $0 \le \hat{z} \le Nh$ where h is the height of each sublayer. The interfaces then lie at $\hat{z} = h,\ 2h,\ 3h,\ \cdots\ (N-1)h$.

The full governing equations for the porous layer are

$$\frac{\partial \hat{u}}{\partial \hat{x}} + \frac{\partial \hat{v}}{\partial \hat{y}} + \frac{\partial \hat{w}}{\partial \hat{z}} = 0, \tag{3}$$

$$\hat{u} = -\frac{K}{\mu}\frac{\partial \hat{p}}{\partial \hat{x}}, \qquad \hat{v} = -\frac{K}{\mu}\frac{\partial \hat{p}}{\partial \hat{y}}, \qquad \hat{w} = -\frac{K}{\mu}\frac{\partial \hat{p}}{\partial \hat{z}} + \frac{\rho \bar{g}\beta K}{\mu}(T - T_{\rm ref}), \tag{4}$$

$$(\rho\mathcal{C})_{\rm pm}\frac{\partial T}{\partial \hat{t}} + \rho\mathcal{C}_f\left(\hat{u}\frac{\partial T}{\partial \hat{x}} + \hat{v}\frac{\partial T}{\partial \hat{y}} + \hat{w}\frac{\partial T}{\partial \hat{z}}\right) = \kappa\left(\frac{\partial^2 T}{\partial \hat{x}^2} + \frac{\partial^2 T}{\partial \hat{y}^2} + \frac{\partial^2 T}{\partial \hat{z}^2}\right), \tag{5}$$

where all quantities are given in the Nomenclature. The boundary and interface conditions are,

$$\hat{z}=0: \qquad \hat{w}=0, \quad T=T_{\rm ref},$$

$$\hat{z}=nh: \qquad \hat{w}=0, \quad T \text{ and } \frac{\partial T}{\partial \hat{z}} \text{ are continuous}, \quad n=1,2,\cdots,N-1, \tag{6}$$

$$\hat{z}=Nh: \qquad \hat{w}=0, \quad T=T_{\rm ref}-N\,\Delta T.$$

These equations and boundary conditions may be made nondimensional by introducing the following scalings,

$$(\hat{x},\hat{y},\hat{z})=h(x,y,z), \qquad \hat{t}=\frac{h^2(\rho\mathcal{C})_{\rm pm}}{\kappa}t, \qquad \hat{p}=\frac{\kappa\mu}{(\rho\mathcal{C})_f K}p,$$
$$(\hat{u},\hat{v},\hat{w})=\frac{\kappa}{h(\rho\mathcal{C})_f}(u,v,w), \qquad T=T_{\rm ref}+\Delta T\,\theta, \tag{7}$$

which are based on the height, h, and the temperature drop, ΔT, corresponding to one sublayer.

The nondimensional equations are now,

$$\frac{\partial u}{\partial x}+\frac{\partial v}{\partial y}+\frac{\partial w}{\partial z}=0, \tag{8}$$

$$u=-\frac{\partial p}{\partial x}, \qquad v=-\frac{\partial p}{\partial y}, \qquad w=-\frac{\partial p}{\partial z}+Ra\,\theta, \tag{9}$$

$$\frac{\partial \theta}{\partial t}+u\frac{\partial \theta}{\partial x}+v\frac{\partial \theta}{\partial y}+w\frac{\partial \theta}{\partial z}=\frac{\partial^2\theta}{\partial x^2}+\frac{\partial^2\theta}{\partial y^2}+\frac{\partial^2\theta}{\partial z^2}, \tag{10}$$

where the Darcy-Rayleigh number is defined to be,

$$Ra=\frac{\rho(\rho\mathcal{C})_f \bar{g}\beta h K\Delta T}{\mu\kappa}. \tag{11}$$

The boundary and interface conditions now become

$$z=0: \qquad w=0, \quad \theta=0,$$

$$z=n: \qquad w=0, \quad \theta \text{ and } \frac{\partial \theta}{\partial z} \text{ are continuous}, \qquad n=1,2,\cdots N-1, \tag{12}$$

$$z=N: \qquad w=0, \quad \theta=-N.$$

Given that we seek to determine whether three-dimensional modes are realizable, we adopt a pressure/temperature formulation of the governing equations. On eliminating the velocities between Eqs. (8) and (9) we obtain the following momentum equation,

$$\nabla^2 p = Ra\,\frac{\partial \theta}{\partial z}, \tag{13}$$

while the heat transport equation becomes,

$$\frac{\partial \theta}{\partial t} = \nabla^2 \theta + \frac{\partial p}{\partial x}\frac{\partial \theta}{\partial x} + \frac{\partial p}{\partial y}\frac{\partial \theta}{\partial y} + \left(\frac{\partial p}{\partial z} - Ra\,\theta\right)\frac{\partial \theta}{\partial z}. \tag{14}$$

The basic state, whose stability characteristics we seek, is given by

$$\theta = -z, \qquad \frac{\partial p}{\partial z} = -Ra\,z, \tag{15}$$

and this applies to all sublayers. The boundary and interface conditions are as before, except that $w = 0$ is replaced by $\dfrac{\partial p}{\partial z} = Ra\,\theta$.

3 Weakly Nonlinear Stability Analysis

It proves convenient to subtract out the basic state given above from the governing equations. Therefore we obtain the following pair of perturbation equations,

$$\nabla^2 P = Ra\,\frac{\partial \Theta}{\partial z}, \tag{16}$$

$$\frac{\partial \Theta}{\partial t} + \frac{\partial P}{\partial z} - Ra\,\Theta = \nabla^2 \Theta + \frac{\partial P}{\partial x}\frac{\partial \Theta}{\partial x} + \frac{\partial P}{\partial y}\frac{\partial \Theta}{\partial y} + \left(\frac{\partial P}{\partial z} - Ra\,\Theta\right)\frac{\partial \Theta}{\partial z}, \tag{17}$$

where we have set $p_z = P_z - Ra\,z$ and $\theta = \Theta - z$, and where P and Θ are the disturbances. The boundary conditions for Θ and P_z at both $z = 0$ and $z = N$ are now homogeneous.

The weakly nonlinear expansion takes the following form,

$$\begin{pmatrix} P \\ \Theta \end{pmatrix} = \epsilon \begin{pmatrix} P_1 \\ \Theta_1 \end{pmatrix} + \epsilon^2 \begin{pmatrix} P_2 \\ \Theta_2 \end{pmatrix} + \epsilon^3 \begin{pmatrix} P_3 \\ \Theta_3 \end{pmatrix} + \cdots, \tag{18}$$

where the small quantity, ϵ, is defined according to,

$$Ra = Ra_0 + \epsilon^2 Ra_2 + \cdots. \tag{19}$$

In the above, Ra_0 is the critical Darcy-Rayleigh number which has been minimised over α, and slightly supercritical conditions are equivalent to positive $O(1)$ values of Ra_2. At successive orders of expansion we obtain the following systems in turn.

At $O(\epsilon)$:

$$\nabla^2 P_1 - Ra_0 \frac{\partial \Theta_1}{\partial z} = 0, \tag{20}$$

$$\nabla^2 \Theta_1 + Ra_0 \Theta_1 - \frac{\partial P_1}{\partial z} = 0. \tag{21}$$

At $O(\epsilon^2)$:

$$\nabla^2 P_2 - Ra_0 \frac{\partial \Theta_2}{\partial z} = 0, \tag{22}$$

$$\nabla^2 \Theta_2 + Ra_0 \Theta_2 - \frac{\partial P_2}{\partial z} = Ra_0 \Theta_1 \frac{\partial \Theta_1}{\partial z} - \nabla P_1 . \nabla \Theta_1. \tag{23}$$

At $O(\epsilon^3)$:

$$\nabla^2 P_3 - Ra_0 \frac{\partial \Theta_3}{\partial z} = Ra_2 \frac{\partial \Theta_1}{\partial z}, \tag{24}$$

$$\nabla^2 \Theta_3 + Ra_0 \Theta_3 - \frac{\partial P_3}{\partial z} = Ra_0 \left(\Theta_1 \frac{\partial \Theta_2}{\partial z} + \Theta_2 \frac{\partial \Theta_1}{\partial z} \right) - \nabla P_1 . \nabla \Theta_2 - \nabla P_2 . \nabla \Theta_1 + \frac{\partial \Theta_1}{\partial \tau} - Ra_2 \Theta_1. \tag{25}$$

In the above, $\tau = \epsilon^2 t$, represents a slow timescale which reflects the fact that disturbances of the form of the neutral mode vary extremely slowly while in the vicinity of the critical Rayleigh number.

At $O(\epsilon)$ the solution is taken to be proportional to the eigensolution corresponding to linear theory at the point in neutral curve where Ra takes its minimum value, Ra_0. As our interest is in the competition between roll solutions and square planforms, we adopt the following solutions at $O(\epsilon)$:

$$\begin{pmatrix} P_1 \\ \Theta_1 \end{pmatrix} = \begin{pmatrix} f_1(z) \\ g_1(z) \end{pmatrix} \left[A e^{i\alpha x} + \overline{A} e^{-i\alpha x} \right] + \begin{pmatrix} f_1(z) \\ g_1(z) \end{pmatrix} \left[B e^{i\alpha (x \cos\phi - y \sin\phi)} + \overline{B} e^{-i\alpha (x \cos\phi - y \sin\phi)} \right], \tag{26}$$

where the modal amplitudes, A and B, are functions only of the slow time scale, τ. The value ϕ is the angle between the rolls, but generally our results will use $\phi = 90°$. The paper by Rees and Genç (2011) provides a very detailed account of the solutions of these equations, although their analysis used dispersion relations and the equations were formulated in terms of the streamfunction rather than the pressure. The equations for f_1 and g_1 are,

$$f_1'' - \alpha^2 f_1 = Ra_0 \, g_1', \tag{27}$$

$$g_1'' - \alpha^2 f_1 + Ra_0 \, g_1 - f_1' = 0, \tag{28}$$

while the boundary and interface conditions are,

$$
\begin{aligned}
z = 0: \qquad & f'_{1,(1)} = 0, \quad g_{1,(1)} = 0, \quad g'_{1,(1)} = 1, \\
z = n: \qquad & f'_{1,(n)} = Ra_0\, g_{1,(n)}, \quad f'_{1,(n+1)} = Ra_0\, g_{1,(n+1)}, \\
& g_{1,(n)} = g_{1,(n+1)}, \quad g'_{1,(n)} = g'_{1,(n+1)}, \qquad n = 1, 2, \cdots N-1, \\
z = N: \qquad & f'_{1,(N)} = 0, \quad g_{1,(N)} = 0.
\end{aligned}
\tag{29}
$$

In the above, the second subscript on f and g refers to the sublayer index. An extra normalising boundary condition ($g'_{1,(1)} = 1$) has also been introduced at $z = 0$ in order to force nonzero solutions. This extra boundary condition means that the system has one boundary/interface condition too many, and therefore the unknown value of Ra may be found by including the extra equation,

$$Ra' = 0. \tag{30}$$

These equations were solved for the present context using a fourth order Runge Kutta scheme coupled with a shooting method. However, a multiple shooting approach was taken where solutions in all sublayers were computed simultaneously and the interface conditions applied as part of that methodology. Thus the above system becomes one of order $4N + 1$ when there are N sublayers. The shooting method then has to determine $4N - 3$ unknown initial conditions.

The process of minimisation with respect to the wavenumber increases the system to one of order $8N + 2$. The very detailed nature of this computation meant that stringent tests for both accuracy of coding and numerical accuracy needed to be undertaken. It was found that the results of Rees and Genç (2011) could be reproduced to any number of decimal places upon decreasing the steplength sufficiently. Therefore we are satisfied that the encoding has been undertaken correctly, particularly since the present formulation uses pressure while that of Rees and Genç (2011) uses the streamfunction to determine a dispersion relation.

Modal interactions of the first order solutions mean that the following substitutions need to be made in order to solve the second order equations:

$$
\begin{aligned}
\begin{pmatrix} P_2 \\ \Theta_2 \end{pmatrix} \; = & \begin{pmatrix} f_2(z) \\ g_2(z) \end{pmatrix} \left[A^2 e^{2i\alpha x} + \text{c.c.} + B^2 e^{2i\alpha(x\cos\phi - y\sin\phi)} + \text{c.c.} \right] + \begin{pmatrix} f_0(z) \\ g_0(z) \end{pmatrix} \left[A\overline{A} + B\overline{B} \right] \\
& + \begin{pmatrix} f_3(z) \\ g_3(z) \end{pmatrix} \left[A\overline{B} e^{i\alpha(x(1-\cos\phi) + y\sin\phi)} + \text{c.c.} \right] + \begin{pmatrix} f_4(z) \\ g_4(z) \end{pmatrix} \left[AB e^{i\alpha(x(1+\cos\phi) - y\sin\phi)} + \text{c.c.} \right].
\end{aligned}
\tag{31}
$$

The f_j and g_j functions ($j = 0, 2, 3, 4$) satisfy the equations,

$$\begin{aligned} &f_2'' - 4\alpha^2 f_2 - Ra_0\, g_2' = 0, \\ &g_2'' + (Ra_0 - 4\alpha^2) g_2 - f_2' = Ra_0\, g_1 g_1' - f_1' g_1' + \alpha^2 f_1 g_1, \end{aligned} \tag{32}$$

$$\begin{aligned} &f_0'' - Ra_0\, g_0' = 0, \\ &g_0'' + Ra_0\, g_0 - f_0' = 2\Big[Ra_0\, g_1 g_1' - f_1' g_1' - \alpha^2 f_1 g_1\Big], \end{aligned} \tag{33}$$

$$\begin{aligned} &f_3'' - \alpha^2(2 - 2\cos\phi) f_3 - Ra_0\, g_3' = 0, \\ &g_3'' + \Big[Ra_0 - \alpha^2(2 - 2\cos\phi)\Big] g_3 - f_3' = 2\Big[Ra_0\, g_1 g_1' - f_1' g_1' - \alpha^2 f_1 g_1 \cos\phi\Big], \end{aligned} \tag{34}$$

$$\begin{aligned} &f_4'' - \alpha^2(2 + 2\cos\phi) f_4 - Ra_0\, g_4' = 0, \\ &g_4'' + \Big[Ra_0 - \alpha^2(2 + 2\cos\phi)\Big] g_4 - f_4' = 2\Big[Ra_0\, g_1 g_1' - f_1' g_1' + \alpha^2 f_1 g_1 \cos\phi\Big]. \end{aligned} \tag{35}$$

All of these equations satisfy the conditions $f_j' = Ra_0\, g_j$ and $g_j = 0$ at both $z = 0$ and $z = N$, and satisfy $f_j' = Ra_0\, g_j$ and continuity of both temperature and temperature gradient at each interface. These latter equations effectively increase the order of the overall system to $(24N + 2)$.

At third order in ϵ a large number of modal interactions arise, but for the purposes of the weakly nonlinear analysis we are interested only in those which yield a term which is proportional to $e^{i\alpha x}$. That part of the $O(\epsilon^3)$ solution which is proportional to $e^{i\alpha x}$ may be found by first using the substitution,

$$\begin{pmatrix} P_3 \\ \Theta_3 \end{pmatrix} = \begin{pmatrix} f_5(z) \\ g_5(z) \end{pmatrix} e^{i\alpha x} + \text{further terms.} \tag{36}$$

The equations for f_5 and g_5 are,

$$f_5'' - \alpha^2 f_5 - Ra_0\, g_5' = ARa_2\, g_1', \tag{37}$$

$$\begin{aligned} &g_5'' + \Big[Ra_0 - \alpha^2\Big] g_5 - f_5' \\ &= (A_\tau - Ra_2 A) g_1 \\ &+ Ra_0\Big[A^2\overline{A}\Big(g_1(g_0' + g_2') + g_1'(g_0 + g_2)\Big) + AB\overline{B}\Big(g_1(g_0' + g_3' + g_4') + g_1'(g_0 + g_3 + g_4)\Big)\Big] \\ &- \Big[A^2\overline{A}\Big(f_1'(g_0' + g_2') + g_1'(f_0' + f_2')\Big) + AB\overline{B}\Big(f_1'(g_0' + g_3' + g_4') + g_1'(f_0' + f_3' + f_4' g)\Big)\Big] \\ &- \alpha^2\Big[2A^2\overline{A}\Big(f_1 g_2 + f_2 g_1\Big) + AB\overline{B}\Big((1 - \cos\phi)(f_1 g_3 + f_3 g + 1) + (1 + \cos\phi)(f_1 g_4 + f_4 g_1)\Big]. \end{aligned} \tag{38}$$

Finally, the solvability condition may be written in the form,

$$\int_0^N \Big[Ra_0\, g_1 \mathcal{R}_1 - f_1 \mathcal{R}_2 \Big]\, dz = 0. \tag{39}$$

Here $\mathcal{R}_1$ and $\mathcal{R}_2$ are the respective inhomogeneous terms in the above equations for f_5 and g_5. With the addition of these solvability conditions a layer consisting of N sublayers is represented by $36N + 5$ first order equations where $36N - 9$ initial conditions are unknown and have to be sought as part of the shooting method. We generally claim at least seven significant figures for the accuracy of our computations for Ω. For large values of N, computational time as well convergence difficulties meant that fewer grid points needed to be used. But in these situations computations with 20 and 40 grid points per sublayer were improved using Richardson's extrapolation formula.

Application of the solvability equations yields an amplitude equation of the form,

$$c_1 \frac{\partial A}{\partial \tau} = c_2 Ra_2 A - A\Big(c_3 A\overline{A} + c_4 B\overline{B} \Big), \tag{40}$$

and, by symmetry since there is rotational invariance, the corresponding equation for B is,

$$c_1 \frac{\partial B}{\partial \tau} = c_2 Ra_2 B - B\Big(c_3 B\overline{B} + c_4 A\overline{A} \Big), \tag{41}$$

where, for a chosen value of N, c_1, c_2 and c_3 are constants while c_4 depends on ϕ. The values of c_1, c_2, c_3 and c_4 are found always to take positive values, and therefore convective onset is always supercritical. In all the cases we tried, c_4 takes its smallest value when the rolls are perpendicular to one another. The detailed analysis of Rees and Riley (1990) (and many other papers) shows that the identity of the postcritical pattern depends on the minimum value of the ratio,

$$\Omega(\phi) = c_4/c_3. \tag{42}$$

For the classical Darcy-Bénard problem, Rees and Riley (1989a) showed that,

$$\Omega = \frac{70 + 28\cos^2\phi - 2\cos^4\phi}{49 - 2\cos^2\phi + \cos^4\phi}, \tag{43}$$

which varies between the maximum of 2 when $\phi = 0$ and the minimum of $10/7$ when $\phi = \pm 90^\circ$. However, values of Ω need to be computed for more complicated configurations, such as the present one.

When $\min_\phi \Omega(\phi) > 1$, then rolls are stable and square cells are unstable to perturbations of the form of one of the constituent rolls. In such situations rolls also transport more heat than do square cells (Rees 2001). The situation is reversed in all respects when $\min_\phi \Omega < 1$ and square cells then form the stable pattern.

4 Results and Discussion

4.1 Rolls or square cells?

The numerical results are given in Table 1, below.

N	Ra_c	α_c/π	$\Omega(90^\circ)$
1	39.478418	1.000000	1.428571
2	27.097628	0.740457	1.625436
3	21.369126	0.595992	1.153075
4	18.728700	0.513106	1.142761
5	17.236333	0.457578	1.136984
6	16.281754	0.416990	1.133008
7	15.619973	0.385630	1.130011
8	15.134656	0.360448	1.127636
9	14.763720	0.339645	1.125695
10	14.471082	0.322080	1.124073
12	14.038961	0.293844	1.121506
16	13.510302	0.254305	1.118036
20	13.199202	0.227374	1.115792
32	12.741069	0.179664	1.112160
40	12.590616	0.160671	1.110871
64	12.367041	0.126993	1.108856
80	12.293076	0.113578	1.108162
100	12.234105	0.101582	1.107598

Table 1: The variation with N of the critical values of Ra and α and the value of the corresponding coupling coefficient, $\Omega(90^\circ)$.

Table 1 show that there is a general trend for the coupling coefficient to decrease as N increases, although the sole exception is when $N = 1$ rises to $N = 2$. This is followed by a sharp drop for $N = 3$, which is the first case for which there is an internal sublayer, and thereafter the decrease is quite sedate. The trend appears to favour a limit which is above 1.0. In the absence of a detailed asymptotic theory for $N \to \infty$ which, if possible for the present problem must be exceptionally complicated, it is reasonable to use the powers of N which appear in Eq. (1) as a guide for a polynomial to fit to the data in Table 1. If a quadratic in $N^{-1/2}$ is chosen, then the data for $N = 64$, 80 and 100 yield the following,

$$\Omega(90^\circ) \sim 1.1050 + 0.007062N^{-1/2} + 0.1923N^{-1}, \tag{44}$$

when N is large. This fit is shown as a dotted line, together with the data given in Table 1, as a function of N^{-1} in Figure 1. Given the relatively small magnitude of the coefficient of $N^{-1/2}$ in Eq. (44), an alternative linear fit in N^{-1} which omits the $N^{-1/2}$ term is

$$\Omega(90^\circ) \sim 1.1053 + 0.22560N^{-1}, \tag{45}$$

which was taken from the $N = 80$ and $N = 100$ data. This fit is also shown in Figure 1 but as a dashed line. The very slight discrepancies between the constant terms in Eqs. (44) and (45) should be resolved by solving for even larger values of N. However, the method of multiple shooting is particularly time-consuming in these extreme situations. As an indication, when $N = 100$, the system being solved consists of 3605 first order equations with 3591 unknown initial conditions. The Newton-Raphson part of the shooting method algorithm then requires the solution of a 3591×3591 matrix/vector system to find the corrections to the unknown initial conditions. However, it is clear that the value $\Omega(90^\circ)$ in the large-N limit is close to 1.105, and this value appears to be very likely to be correct to four significant figures. Therefore roll cells, rather than convection with a square planform, will be preferred.

We note that the three-layer system which was considered by Riahi (1983), in which a central porous layer was surrounded by conducting regions of infinite extent, does admit square cell solutions in some cases. The analysis of Rees and Mojtabi (2011) also finds this for situations where the bounding conducting layers are of finite thickness. Therefore it is quite possible that if the present assumption of having infinitesimally thin interfaces is relaxed, (such as has been considered in the recent detailed multilayer linear analysis by Patil and Rees (2014) and earlier by Jang and Tsai (1988) and Postelnicu (1999)) then this could provide a means by which square cells could be preferred in a multilayered system.

4.2 The coupling coefficient for general values of ϕ

As a final check on the conclusion that rolls are preferred over square cells, this subsection considers briefly how Ω varies with ϕ. We have seen above that Ω achieves a maximum of 2 when $\phi = 0$ and a minimum of 10/7 when $\phi = 90^\circ$ for the single layer case. Figure 2 shows the corresponding curves for $N = 2$, 3, 4, 5, 10, 20 and 40. In all cases $\Omega(0) = 2$ and Ω decreases monotonically as ϕ increases towards 90°, at which point we recover the values given in Table 1, and they clearly represent the minimum value for each N. Therefore it is concluded that there is no situation for which Ω achieves a value which is less than 1, and hence rolls persist.

5 Conclusions

To summarise briefly, in this short paper we have provided a weakly nonlinear theory for convection in a layered system consisting of identical porous sublayers with infinitesimally thin but impermeable interfaces. The onset conditions found using the present pressure/temperature formulation are identical to those obtained by Rees and Genç using a dispersion relation based on a streamfunction/temperature formulation. Of prime interest is the value of the coupling coefficient, Ω, which is a function both of ϕ, the relative orientation of two rolls and N, the number of sublayers. Ω takes its smallest value in all cases when the rolls are perpendicular, and although $\Omega(90^\circ)$ decreases as N increases (for $N > 2$), it appears to approach the value 1.105. Being about 1 this means that roll cells will always be favoured immediately post onset.

REFERENCES

Jang, J.Y., Tsai, W.L.: Thermal instability of two horizontal porous layers with a conductive partition. Int. J. Heat Mass Transfer **31**, 993-1003 (1988).

Newell, A.C., Whitehead, J.A.: Finite bandwidth, finite amplitude convection. J. Fluid Mech. **38**, 279-303 (1969).

Nield, D.A., Bejan, A.: Convection in Porous Media (4th edition), Springer, New York (2012).

Patil, P.M., Rees, D.A.S.: The onset of convection in a porous layer with multiple horizontal solid partitions. International Journal of Heat and Mass Transfer **68**, 234-246 (2014).

Postelnicu, A.P.: Thermal stability of two fluid porous layers separated by a thermal barrier. *Proceedings of the 3rd Baltic Heat Transfer Conference*, Gdansk, Poland, pp. 443-450, (1999).

Rees, D.A.S.: The stability of Darcy–Bénard convection. Handbook of Porous Media ed. K.Vafai. (Marcel Dekker), pp.521–558, (2000).

Rees, D.A.S.: Stability analysis of Darcy-Bénard convection. Lecture notes for the *Summer School on Porous Medium Flows*, Neptun, Constanţa, Romania (25-29 June 2001).

Rees, D.A.S., Genç, G.: The onset of convection in porous layers with multiple horizontal partitions. Submitted to: International Journal of Heat and Mass Transfer (2010).

Rees, D.A.S., Mojtabi, A.: The effect of conducting boundaries on weakly nonlinear Darcy-Bénard convection. Transport in Porous Media **88**, 45-63 (2011).

Rees, D.A.S., Riley, D.S.: The three-dimensional stability of finite-amplitude convection in a layered porous medium heated from below. J. Fluid Mech **211**, 437-461 (1990).

Riahi, N.: Nonlinear convection in a porous layer with finite conducting boundaries. J. Fluid Mech **129**, 153-171 (1983).

Tyvand, P.A.: Onset of Rayleigh-Bénard Convection in Porous Bodies. Transport Phenomena in Porous Media II, eds. Ingham, D.B., Pop, I., Elsevier, New York, pp. 82–112, (2002).

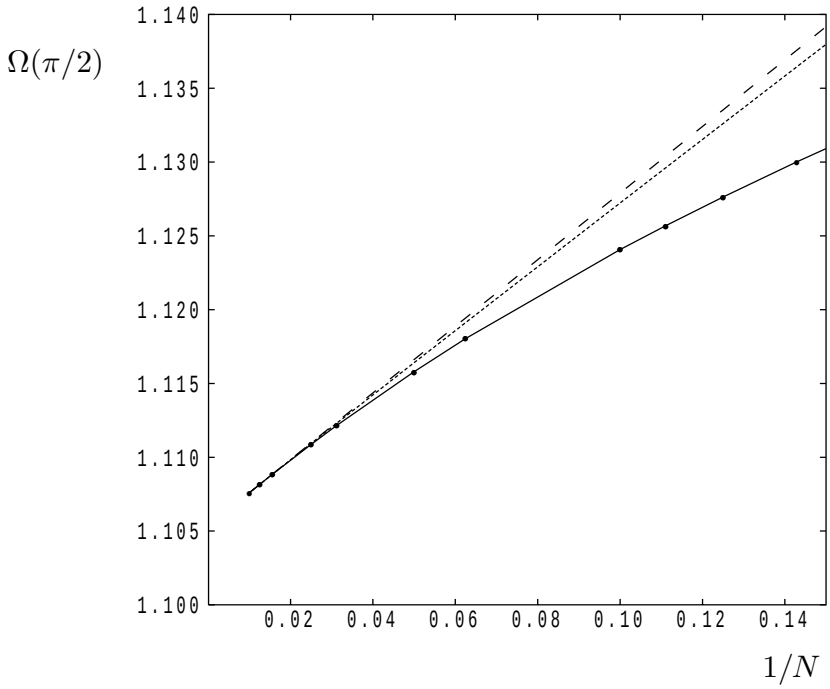

Figure 1: The variation of $\Omega(\pi/2)$ with N^{-1}. Bullets denote the data from Table 1 which are joined by the continuous line. The dotted line represents Eq. (44) while the dashed line represents Eq. (45).

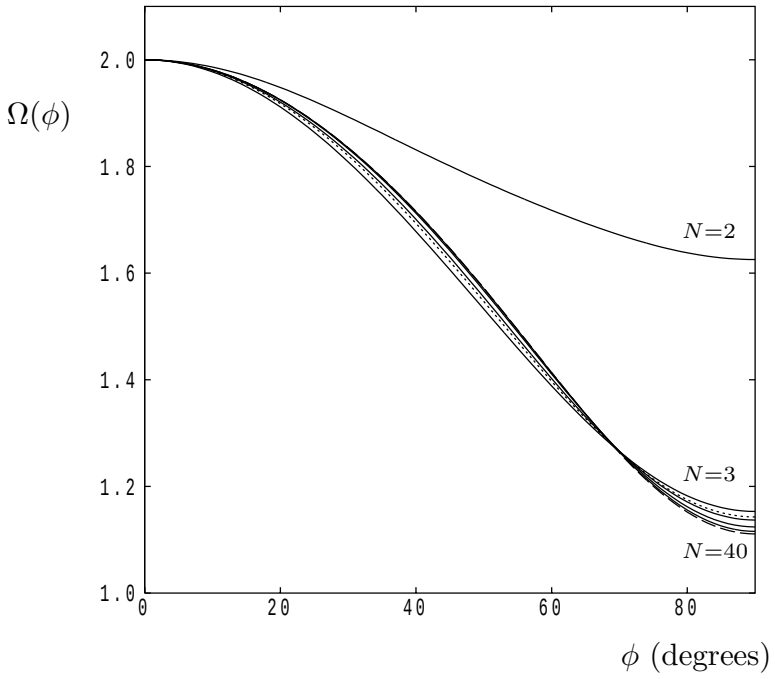

Figure 2: Displaying the variation of $\Omega(\phi)$ with ϕ for $N = 2$, 3, 4, 5, 10, 20 and 40.